Modeling of Power Efficiency in a Magnetohydrodynamic Generator

By
Michael Redle

A THESIS

submitted to

Oregon State University

University Honors College

in partial fulfillment of
the requirements for the
degree of

Honors Baccalaureate of Science in Mathematics
(Honors Scholar)

Presented May 29, 2018
Commencement June 2018

AN ABSTRACT OF THE THESIS OF

Michael Redle for the degree of Honors Baccalaureate of Science in Mathematics
presented on May 29, 2018. Title:
Modeling of Power Efficiency in a Magnetohydrodynamic Generator

Abstract approved:

Nathan L. Gibson

The introduction of an Magnetohydrodynamic (MHD) generator in coal or natural gas energy plants could significantly increase the efficiency by converting kinetic and thermal energy of the combustion exhaust to electrical energy by the generation of a Faraday and Hall current. The traditional MHD system was transformed into a simplified MHD model using assumptions that are reasonable in applications. To find a solution to the simplified model, backward finite difference method was implemented. The solutions to the model were then used in a constrained numerical optimization to maximize efficiency as a function of various initial conditions such as velocity, temperature, and pressure.

Key Words: Magnetohydrodynamics, Optimization, Power Generation

Corresponding e-mail address: redlem@oregonstate.edu

Modeling of Power Efficiency in a Magnetohydrodynamic Generator

By
Michael Redle

A THESIS

submitted to

Oregon State University

University Honors College

in partial fulfillment of
the requirements for the
degree of

Honors Baccalaureate of Science in Mathematics
(Honors Scholar)

Presented May 29, 2018
Commencement June 2018

Honors Baccalaureate of Science in Mathematics project of Michael Redle presented on May 29, 2018

APPROVED:

Nathan L. Gibson, Mentor, representing the Department of Mathematics

---

Vrushali A. Bokil, Committee Member, representing the Department of Mathematics

---

C. Rigel Woodside, Committee Member, representing National Energy Technology Laboratory

---

Toni Doolen, Dean, Oregon State University Honors College

I understand that my project will become part of the permanent collection of Oregon State University Honors College. My signature below authorizes release of my project to any reader upon request.

Michael Redle, Author

Contents

1 Introduction **2**

2 MHD Power Generation **3**

3 Derivations of MHD Equations **4**

3.1 Conservation of Momentum Equation 4

3.2 Energy Conservation Equation 8

3.3 Conclusion of Derivations 11

4 System of Simplified MHD Equations **12**

5 Numerical Methods **21**

6 Numerical Solution **26**

7 Optimization of Efficiency **32**

8 Conclusion **37**

1 Introduction

Magnetohydrodynamics is the study of how a magnetic field interacts with electrically conducting fluids such as plasmas, liquid metals, salt water, and electrolytes, and is a naturally occurring phenomena in solar winds, solar flares, and in the generation of magnetic fields in planets and stars [7]. Such phenomena can be engineered for power generation via a Magnetohydrodynamic (MHD) generator, which is a system that transforms kinetic and thermal energy of a conductive fluid into electricity by the implementation of a magnetic field. This generator may be implemented into a coal or natural gas power plant system to increase the extraction of electrical power [7], possibly raising efficiencies from 40% to about 60% or more [4, p. 4]. This large increase in efficiency would allow those power plants to create more energy off of less fuel, thus decreasing cost of energy production, but also decreasing carbon dioxide emissions into the atmosphere.

Our main objective is to investigate the improvement of power efficiency using simulation based optimization which requires efficient forward models. This thesis will begin with the basics of how the MHD generator works, along with the derivations of the general MHD equations. Next, we will describe the simplified system of equations that will be used in our model, followed by our numerical setup and solutions to these equations, along with the optimization of efficiency problem. We will conclude with a discussion of our results, how this model is directly related to that that would be implemented into combustion-based power plant systems, and future directions.

2 MHD Power Generation

An MHD generator requires an applied magnetic field and a moving conductive fluid to generate an electrical current that is extracted by electrodes. The electrodes are placed according to the direction of the applied magnetic field $\mathbf{B}$ and the velocity of the conductive fluid $\mathbf{v}$, since the electric current generated (known as the Faraday current) is in the direction $-\mathbf{v} \times \mathbf{B}$. We consider a high velocity MHD generator, which is advantageous to increase the magnitude of the Lorentz force $\mathbf{F} = q(\mathbf{E} + \mathbf{v} \times \mathbf{B})$, thus increasing the conduction current $\mathbf{j}$ described by the generalized Ohm's law:

$$\mathbf{j} = \sigma\Big[\mathbf{E} + \mathbf{v} \times \mathbf{B} - \beta(\mathbf{j} \times \mathbf{B})\Big],$$

where σ is conductivity, $\mathbf{E}$ is the electric field, and β is the hall parameter. High temperatures are desirable in gas driven MHD generators since conductivity is typically negligible except at high temperatures [4, p. 2].

Scientists have found fairly simple ways to implement the high temperature and magnetic fields, and this gives insight of why a combustion plant would be ideal, for the exhaust of combustion can be at high enough temperatures to produce a plasma if the oxidant concentration (O_2 concentration in air is only about 20%) is increased or additional air-preheating is done. The implementation of a higher velocity is more difficult in applications – it requires a convergent-divergent channel that would force transient flow, or make the exhaust enter this channel at subsonic speeds and leave at

supersonic speeds. When a plasma flows through an MHD generator with the above criteria, an electrical current is produced.

3 Derivations of MHD Equations

This section will contain the derivations of the MHD equations available in the literature. These equations will describe the setting within that of an MHD generator. It will also include simplifications of these equations, which will be used for our problem at hand. Note that these derivations and simplifications were originally done in Sutton and Sherman et al., and are summarized within this paper as background. In addition, many of these derivations will start on the microscopic, chemical species scale, which will lead to a macroscopic system of equations that has a reduced dependence of individual chemical species.

3.1 Conservation of Momentum Equation

For conservation of momentum, our derivation will begin with the Maxwell transport equation [6, p. 112]:

$$\frac{\partial}{\partial t}(n_s\langle\Theta\rangle_s) + \nabla\cdot(n_s\langle\Theta\mathbf{w}\rangle_s) - \frac{n_s}{m_s}\langle\mathbf{F}_s\cdot\nabla_w\Theta\rangle_s = \int\Theta_s\Big(\frac{\partial f}{\partial t}\Big)d\mathbf{w}, \tag{1}$$

where

$\mathbf{w}$ = particle velocity with respect to surroundings,

$\mathbf{F}_s$ = Force on a particle species,

Θ = some molecular property, which can be chosen (i.e. mass, charge, energy, etc.),

f = velocity distribution function,

m_s = particle mass of a species,

n_s = number density of a particle species,

$\langle \cdots \rangle$ = average,

$\mathbf{ab}$ = dyad, $D(\mathbf{a}, \mathbf{b})$ [3].

Now let Θ be equal to the momentum of a single species, that is, let $\Theta = m_s\mathbf{w}$ [6, p. 113]. This modifies equation (1) to

$$\frac{\partial}{\partial t}(\rho_s\langle \mathbf{w} \rangle_s) + \nabla \cdot (\rho_s\langle \mathbf{ww} \rangle_s) - n_s\langle (\mathbf{F}_s \cdot \nabla_w)\mathbf{w} \rangle_s = \int m_s\mathbf{w}\Big(\frac{\partial f}{\partial t}\Big)d\mathbf{w}, \qquad (2)$$

with ρ_s being the mass density of the species. This can be simplified as follows [6, p.

113]:

$$\left\langle \mathbf{w} \right\rangle_s = \mathbf{v}_s, \tag{3a}$$

$$\left\langle \mathbf{ww} \right\rangle_s = \mathbf{vv} + \mathbf{vV_s} + \mathbf{V_s v} + \left\langle \mathbf{cc} \right\rangle_{\mathbf{s}}, \tag{3b}$$

$$\rho_s \left\langle \mathbf{cc} \right\rangle_s = \mathbf{p}_s, \tag{3c}$$

$$\mathbf{F_s} \cdot \nabla_{\mathbf{w}} \mathbf{w} = \mathbf{F_s}, \tag{3d}$$

$$\left\langle \mathbf{F} \right\rangle_s = eZ_s \left\langle \mathbf{E}^* + \mathbf{V_s} \times \mathbf{B} \right\rangle_{\mathbf{s}}, \tag{3e}$$

with:

$\mathbf{v_s}$ = mean velocity of a species,

$\mathbf{v}$ = mean velocity,

$\mathbf{V_s}$ = diffusion/drift velocity vector,

$\mathbf{c} = \mathbf{w} - \mathbf{v}$ = particle random thermal velocity,

e = sum of internal and thermal energy per unit mass,

Z = number of charges of species s,

$\mathbf{E}^*$ = electric field in coordinates moving with mass average gas velocity,

$\mathbf{B}$ = magnetic induction,

$\mathbf{p}_\mathrm{s}$ =pressure tensor.

The equations in (3) now imply

$$\frac{\partial}{\partial t}(\rho_s \mathbf{v}_s)+\nabla\cdot[\rho_s(\mathbf{v}\mathbf{V_s}+\mathbf{V_s}\mathbf{v})]+\nabla\cdot(\rho_s\mathbf{v}\mathbf{v})+\nabla\cdot\mathbf{p}_s=\mathbf{P}_s(m\mathbf{w})+n_seZ_s(\mathbf{E}^*+\mathbf{V_s}\times\mathbf{B}), \tag{4}$$

with $\mathbf{P_s}$ being the dynamical friction vector of species [6, p. 114]. To obtain the overall momentum equation, equation (4) must be summed over all species. Note that by definition, $\sum_s \rho_s \mathbf{V_s} = 0$, and due to conservation of momentum, $\sum_s \mathbf{P_s} = 0$ as well [6, p. 114]. Also, summing the pressure tensor over all species becomes total pressure tensor $\mathbf{p}$ [6, p. 114]. Therefore, equation (4) becomes

$$\frac{\partial}{\partial t}(\rho_s \mathbf{v}_s) + \nabla\cdot(\rho_s\mathbf{v};\mathbf{v}) + \nabla\cdot\mathbf{p} = \mathbf{E}^*\sum_s n_seZ_s + \sum_s n_seZ_s\mathbf{V}_s\times\mathbf{B}. \tag{5}$$

Next, the net charge defined as $\sum_s n_seZ_s = \rho_e$, where ρ_e is the charge density, is typically very small in a plasma, and therefore can be be neglected [6, p. 115]. In addition, the second term on the right can be rewritten since $\mathbf{j} = \sum_s n_seZ_s\mathbf{V_s}$. Also the expansion and simplification of the left term in equation (5) shows it is equivalent to $\rho\frac{D\mathbf{v}}{Dt}$. The last adjustment that will be made is to rewrite the pressure tensor into the sum of the stress tensor $\vec{\tau}$ and the hydrostatic pressure, or $\mathbf{p} = \boldsymbol{\tau} + p\mathbf{l}$. With these simplifications, the overall momentum equation becomes [6, p. 115]

$$\rho\frac{D\mathbf{v}}{Dt} = -\nabla\cdot\tau - \nabla p + \mathbf{j}\times\mathbf{B}. \tag{6}$$

This can be rewritten to give the final conservation of momentum equation for the plasma travelling in an MHD generator:

$$\rho \frac{D\mathbf{v}}{Dt} = \psi - \nabla p + \mathbf{j} \times \mathbf{B}, \tag{7}$$

with ψ being the viscous force vector and $\mathbf{j}$ being the conduction current vector.

3.2 Energy Conservation Equation

The Maxwell Transport equation will be the starting point for the derivation of the equation for energy conservation, but instead of evaluating the transport equation with the molecular property Θ_s being the momentum of a molecule, let Θ_s be the particle energy with respect to the laboratory, that is, define Θ_s as follows [6, p. 116]:

$$\Theta_s = \epsilon = \frac{1}{2} m_s w^2 + \epsilon_{int}, \tag{8}$$

where ϵ_{int} is the internal energy of a particle and w is the magnitude of the velocity with respect to the laboratory. We then receive the first average needed for the energy conservation equation by taking the average of the species energy, so it can be evaluated in the transport equation, and by applying the definition of partial pressure and the "peculiar" energy of the species [6, p. 116],

$$\langle \Theta \rangle_s = \frac{1}{2} m_s v^2 + m_s \sum_k v_k V_{k^s} + \langle \epsilon_{tr} \rangle_s + \langle \epsilon_{int} \rangle_s. \tag{9}$$

Next, Θw_i in the Maxwell transport is defined as follows for the energy conservation equation [6, p.117]

$$\Theta w_i = \frac{1}{2} m_s w_k^2 w_i + w_i \epsilon_{int}^s.$$

Following the substitution of $\mathbf{w} = \mathbf{v} + \mathbf{c}$, where $\mathbf{v}$ is the mean velocity vector and $\mathbf{c}$ is the particle random thermal velocity vector, then taking the average and rearranging yields equation (10) [6, p. 117],

$$\langle \Theta w_i \rangle_s = v_i \Big(\frac{1}{2} m_s v^2 + \frac{1}{2} m_s \langle c^2 \rangle_s + \langle \epsilon_{int} \rangle_s \Big) + \Big\langle c_i \big(\frac{1}{2} m_s c^2 + \epsilon_{int} \big) \Big\rangle + \frac{1}{2} m_s v^2 V_{i^s} + m_s v_i (\mathbf{v} \cdot \mathbf{V_s}) + m_s \sum_k v_k \langle c_i c_k \rangle_s. \tag{10}$$

This can be further simplified due to a few definitions: First, the 2 terms $\frac{1}{2} m_s \langle c^2 \rangle_s + \langle \epsilon_{int} \rangle_s$ are equal to the species peculiar energy $\langle \epsilon \rangle_s$. Second, we may substitute the molecular transport of peculiar energy $\langle c_i (\frac{1}{2} m_s c^2 + \epsilon_{int}) \rangle$ with the equivalent heat flux vector, defined by q_i^s / n_s. In addition, we may use the definition for the pressure tensor $p_{ik}^s = n_s m_s \langle c_i c_k \rangle_s$ to substitute for the summation term. Following these simplifications returns the equation below [6, p.117]:

$$\langle \Theta w_i \rangle_s = v_i \Big(\frac{1}{2} m_s v^2 + \langle \epsilon_s \rangle_s \Big) + \frac{q_i^s}{n_s} + \frac{1}{2} m_s v^2 V_i^s + m_s v_i (\mathbf{v} \cdot \mathbf{V_s}) + \frac{v_k p_{ik}}{n_s}. \tag{11}$$

Lastly, to evaluate the force term in the Maxwell transport equation from equation (8), we can define the gradient $\nabla_w \Theta = \partial \Theta / \partial w_i$ to be $m_s w_i$. This, along with the

definition of the force, given by $F_i = eZ(E_i + w_j B_k - w_k B_j)$, gives us the following definition [6, p. 118]:

$$\begin{aligned}\sum_i \frac{F_i}{m_s}\left(\frac{\partial \Theta}{\partial w_i}\right) &= eZ_s(\mathbf{E} + \mathbf{w} \times \mathbf{B})\cdot\mathbf{w} \\ &= eZ_s\mathbf{E}\cdot\mathbf{w}. \end{aligned} \tag{12}$$

Taking the average over the species, we receive the simplification of the third term in the Maxwell Transport Equation,

$$\begin{aligned} n_s\left\langle \sum_i \frac{F_i}{m_s}\left(\frac{\partial \Theta}{\partial w_i}\right)\right\rangle_s &= eZ_s\mathbf{E}\cdot\langle\mathbf{w}\rangle_s \\ &= n_s eZ_s\mathbf{E}\cdot\mathbf{v}_s. \end{aligned} \tag{13}$$

Compiling equations (9), (11), (13), and simplifying with the electric current vector in relation to a species $\mathbf{J}_s = n_s eZ_s\mathbf{v}_s$, the mass density of a species $\rho_s = n_s m_s$, and the mass definition of the species peculiar energy $\langle\epsilon\rangle_s = e_s m_s$, we receive the conservation of energy equation in relation to each individual species [6, p. 118],

$$\begin{aligned}\frac{\partial}{\partial t}\rho_s\Big(\frac{1}{2}v^2 + \mathbf{v}\cdot\mathbf{V}_s + e_s\Big) + \nabla\cdot\rho_s\Big(\frac{1}{2}v^2 + e_s\Big)\mathbf{v} + \nabla\cdot\mathbf{q}_s \\ + \nabla\cdot\rho_s\Big[\frac{1}{2}v^2\mathbf{V}_s + \mathbf{v}(\mathbf{v}\cdot\mathbf{V})_s\Big] + \nabla\cdot(\mathbf{v}\cdot\mathbf{p}_s) = \mathbf{E}\cdot\mathbf{J}_s + \int \epsilon_t\Big(\frac{\partial f}{\partial t}\Big)_c d\mathbf{w}. \end{aligned} \tag{14}$$

Summing equation (14) over all chemical species, noting again the definition $\sum_s \rho_s \mathbf{V}_s = 0$, gives the conservation of energy equation [6, p. 119],

$$\frac{\partial}{\partial t}\Big[\rho\Big(\frac{1}{2}v^2 + e\Big)\Big] + \nabla \cdot \Big[\rho\Big(\frac{1}{2}v^2 + e\Big)\mathbf{v}\Big] + \nabla \cdot \mathbf{q} + \nabla \cdot (\mathbf{v} \cdot \mathbf{p}) = \mathbf{E} \cdot \mathbf{J}. \tag{15}$$

It is more convenient to write equation (15) for the total enthalpy $H = \frac{1}{2}v^2 + e + p/\rho$, where p is the hydrostatic pressure [6, p. 120]. By summing the first 2 terms of the equation, then simplifying and applying the definition of a full derivative and that $\nabla \cdot (\mathbf{v} \cdot \mathbf{p}) = \nabla \cdot p\mathbf{v} + \nabla \cdot (\mathbf{v} \cdot \boldsymbol{\tau})$, then our energy equation becomes [6, p. 121]:

$$\rho \frac{D}{Dt}\Big(\frac{1}{2}v^2 + e\Big) = -\nabla \cdot \mathbf{q} - \nabla \cdot p\mathbf{v} - \nabla \cdot (\mathbf{v} \cdot \boldsymbol{\tau}) + \mathbf{E} \cdot \mathbf{J}. \tag{16}$$

We then can change variables by applying $H - p/\rho = \frac{1}{2}v^2 + e$ and simplifying to give the time dependent conservation of energy equation,

$$\rho \frac{DH}{Dt} - \frac{\partial p}{\partial t} = -\nabla \cdot \mathbf{q} - \nabla \cdot (\mathbf{v} \cdot \boldsymbol{\tau}) + \mathbf{E} \cdot \mathbf{J}. \tag{17}$$

3.3 Conclusion of Derivations

Understanding the derivations and assumptions for the conservation of momentum and energy equations lend an understanding to the MHD equations. For our model, we will use equations (7) and (17) and modify to get to a system of equations that will then be created in to a simulation, and then optimized, which we be described

further in the following section.

4 System of Simplified MHD Equations

To close the final system of equations, we will follow steps within Sutton and Sherman et al. along with some further simplifications and assumptions. We want our system to represent a 1-Dimensional steady state MHD generator that can allow for heat loss and drag effects. Although this is not a perfect representation of what is happening in an MHD generator, it is a reasonable simplification since the velocity in the x direction in an open cycle generator is significantly larger than that of both the y and z directions [6, p. 393]. Also, the steady state assumption is perfectly reasonable since a constant flow of fluid can be used in applications of an MHD generator. These simplifications imply the following [6, p. 393]:

$$\frac{\partial}{\partial t} = \frac{\partial}{\partial y} = \frac{\partial}{\partial z} = 0,$$

$$v = w = 0,$$

where v is the velocity in the y direction and w is the velocity in the z direction. This then modifies the conservation of momentum equation (7) to

$$\rho u \frac{du}{dx} = \psi - \frac{dp}{dx} + (\mathbf{j} \times \mathbf{B})_x. \tag{18}$$

Since the applied magnetic field is significantly larger than the induced magnetic field, or $\mathbf{B_A} >> \mathbf{B_I}$, then $\mathbf{B} = \mathbf{B_A} + \mathbf{B_I} \approx \mathbf{B_A}$, or the whole magnetic field is about the same as the applied field, which is constant in applications. Therefore, we will let $\mathbf{B} \approx B_z(x) = B_z$, which removes any time derivatives in the Maxwell equations used in the general MHD equations. Also the conduction current $\mathbf{j}$ is dependent on $\mathbf{E}$, the electric field, which is dependent on the induced magnetic field. Thus, the above simplification of $\mathbf{B_I} \approx 0$ implies $E_x \approx 0$, thus simplifying equation (18) to

$$\rho u \frac{du}{dx} = \psi - \frac{dp}{dx} + j_y B_z. \tag{19}$$

We will then substitute the viscous force vector ψ, or the drag component of this equation, with an enhancement factor representing drag [6, p. 500]. The enhancement factor used is the friction pressure drop, or μ, which is defined as [6, p. 500]:

$$\mu = -\frac{\tau_w C}{A},$$

with

τ_w = Shear stress at wall of the channel,

C = perimeter of channel cross section,

A = Area of channel cross section.

We can also apply the definition of the skin friction coefficient $c_f = \frac{2\tau_w}{\rho u^2}$ [6, p. 499],

and rearrange the enhancement factor μ to be

$$\mu = -\frac{\rho u^2 c_f C}{2A}.$$

This definition can then be used within the conservation of momentum equation, thus giving the first of our system of equations,

$$\boxed{\rho u \frac{du}{dx} = \mu - \frac{dp}{dx} + j_y B_z,} \tag{20}$$

with the pressure to be defined as an ideal gas, or $p = \rho RT$. We can also apply our steady state and 1-dimensional simplifications to the conservation of energy equation, along with applying a simplification for heat transfer through the walls of the channel, or apply $-\nabla \cdot \mathbf{q} = q_w \frac{C}{A} = h(T_s - T_w)\frac{C}{A}$, where h is the film coefficient, T_s is the bulk-gas stagnation temperature, and T_w is the temperature of the wall [6, p. 500]. This along with assuming $-\nabla \cdot (\mathbf{v} \cdot \boldsymbol{\tau}) = 0$, and that the electric field in the x and z directions are zero due to the magnitude of the applied magnetic field gives the conservation of energy equation that we will use in our system,

$$\boxed{\rho u \frac{dH}{dx} = E_y j_y - h(T_s - T_w)\frac{C}{A}.} \tag{21}$$

We will close our system of nonlinear differential equations by defining the remaining parameters. First, during the gaseous flow through the MHD generator, it would be ideal in applications to have the magnetic field $\mathbf{B} = B_z$ and the mass flow rate $\dot{\mathbf{m}}$

held constant so there is no abnormal fluctuation. Let the mass flow rate be defined by the following conservation of mass equation [4, p. 136],

$$\rho = \frac{\dot{\mathbf{m}}}{Au}. \tag{22}$$

As we said before, because the magnetic field can be simplified to only be in the z direction, we can simplify $E_z = 0$. Also, in previous research, it has previously been found that a segmented Faraday electrode set up was optimal choice, which will be applied to our system [4, p. 158]. This segmented Faraday electrode system has been found to have an electric field defined as [4, p. 10]:

$$E_y = uB_z(1 - K), \tag{23}$$

$$E_x = 0, \tag{24}$$

where K is defined as the load factor. We will also define our conduction current $\mathbf{j}$ again by the generalized Ohm's law [4, p. 29]:

$$\mathbf{j} = \sigma\Big[\mathbf{E} + \mathbf{v} \times \mathbf{B} - \beta(\mathbf{j} \times \mathbf{B})\Big], \tag{25}$$

where σ is the conductivity and β is the hall parameter. This may be simplified

following our 1-dimensional approximations [6, p. 393]:

$$j_y = \frac{\sigma}{1+(\omega\tau)^2}\Big[E_y - uB_z + \omega\tau E_x\Big], \tag{26}$$

$$j_x = \frac{\sigma}{1+(\omega\tau)^2}\Big[-\omega\tau(E_y - uB_z)\Big], \tag{27}$$

where $\omega\tau = \beta = \frac{\sigma B_z}{en_e}$ by definition, e is defined as the charge of an electron, and n_e is defined as the number density of electrons per cubic meter. After our 1 dimensional simplifications, we can see that j_x is not used in our system of differential equations because it is canceled in both $(\mathbf{j}\times\mathbf{B})_x$ of equation (18) and in $\mathbf{E}\cdot\mathbf{J}$ of equation (17). We then can define the conductivity used in j_y, which includes the electron collision term, by the definition offered by Rosa [4, p. 25]:

$$\sigma = \frac{n_e e^2}{m_e c_e}\left[\frac{1}{\sum_k n_k Q_k + 3.9 n_i\left(\frac{e^2}{8\pi\epsilon_0 kT}\right)^2 \ln\Lambda}\right], \tag{28}$$

$$\Lambda = \frac{12\pi}{n_e^{1/2}}\left(\frac{\epsilon_0 kT}{e^2}\right)^{3/2}, \tag{29}$$

$$c_e = \sqrt{\frac{8kT}{\pi m_e}}, \tag{30}$$

$$n_k = \rho\frac{m_k}{m_{tot}}\frac{1}{m_k^a}, \tag{31}$$

where:

c_e = thermal velocity,

k = Boltzmann constant,

m_k = mass of species k,

m_{tot} = total mass,

m_e = mass of electron,

m_k^a = atomic mass of species k,

n_k = number density of corresponding molecular species,

Q = Collision Cross section of corresponding molecular species,

ϵ_0 = Permittivity of free space,

n_i = number density of ions.

Note that if there is a large percentage of molecules being ionized, then the n_i term, or the electron collision term, dominates. We then will simplify the plasma in the system to be solely compromised of Argon and Cesium, with Cesium contributing the large percentage of the electrons. This further simplifies our conductivity,

$$\sigma = \frac{n_e e^2}{m_e c_e}\left[\frac{1}{n_{Ar}Q_{Ar} + n_{Cs}Q_{Cs} + 3.9n_i\left(\frac{e^2}{8\pi\epsilon_0 kT}\right)^2 \ln\Lambda}\right]. \tag{32}$$

With the approximation that only Cesium atoms will ionize, we then can represent the number density of electrons by a first ionization level simplification of Saha's equation [5, p. 63]:

$$\frac{\alpha^2}{1-\alpha} = 2\frac{s_1}{s_0}\frac{1}{n_{Cs}\rho}\left(\frac{2\pi m_e kT}{h^2}\right)^{3/2} e^{-I_1/kT}, \tag{33}$$

$$n_e = \alpha n_{Cs}, \tag{34}$$

with

$s = \sum_m e^{\frac{-I_m}{kT}}$ = Electron partition function,

I_m = the excitation energy of a Cs ion in the m^{th} state,

h = Planck's constant.

This simplification works while the temperature is relatively low, or less than about 7,000-8,000 Kelvin, otherwise atoms Argon will ionize as well and Cesium could be doubly ionized [5, p. 69]. We will then define the temperature and the stagnation temperature T_s, which will be used in the conservation of energy equation (21). Temperature is defined from the definition of specific enthalpy being the sum of kinetic energy added to the heat exchange per kilogram,

$$T = \frac{H - \frac{1}{2}u^2}{C_{Ar}}, \tag{35}$$

$$T_s = T + \frac{u^2}{2C_{Ar}}. \tag{36}$$

Note that we are using C_{Ar} in this temperature definition since in theory, more than 95% of our system will be Argon. Lastly, to close our system we will impose initial conditions on the channel. In applications, we can shape the channel and increase the flow rate depending on the size and shape of the channel, but in our case we want to choose the best shape of channel to fit optimal conditions of power efficiency. It

is recommended by Rosa et al. that a channel be devised to have a constant Mach number, or $1 < M = u/c_e$, and this argument is used for a lot of discussion throughout the book [4, p. 39]. To implement this, our system will have a fixed Mach number throughout the channel and will solve for the area on each spatial step accordingly to fit equation (22). We can then calculate the initial velocity we would need to implement based off of the chosen Mach number, and can implement a desired initial mass flow rate, pressure, and temperature. Determination of these initial conditions on our systems will be discussed further in the optimization of efficiency section. Note that we can calculate the initial enthalpy from temperature and velocity, thus closing our system. The full system of equations is outlined below:

$$\rho u \frac{du}{dx} = -\frac{dp}{dx} + j_y B_z + \mu, \tag{37a}$$

$$\rho u \frac{dH}{dx} = E_y j_y - \frac{q_w C}{A}, \tag{37b}$$

$$p = \rho R T, \tag{37c}$$

$$T = \frac{H - \frac{1}{2}u^2}{C_{Ar}}, \tag{37d}$$

$$M = u/c_e, \tag{37e}$$

with the following initial conditions:

$$M(0) = M_0, \tag{38a}$$

$$T(0) = T_0, \tag{38b}$$

$$p(0) = p_0, \tag{38c}$$

$$\dot{m} = \dot{\mathbf{m}}(x) = \dot{\mathbf{m}}_0, \tag{38d}$$

and the following parameters used within the system:

$$\rho = \frac{\dot{m}}{Au}, \tag{39a}$$

$$\mu = -\frac{1}{2}\rho u^2 c_f \frac{C}{A}, \tag{39b}$$

$$j_y = \frac{\sigma}{1+(\omega\tau)^2}\Big[E_y - uB_z + \omega\tau E_x\Big], \tag{39c}$$

$$\sigma = \frac{n_e e^2}{m_e c_e}\left[\frac{1}{n_{Ar}Q_{Ar} + n_{Cs}Q_{Cs} + 3.9n_i\Big(\frac{e^2}{8\pi\epsilon_0 kT}\Big)^2 \ln\Lambda}\right], \tag{39d}$$

$$\Lambda = \frac{12\pi}{n_e^{1/2}}\Big(\frac{\epsilon_0 kT}{e^2}\Big)^{3/2}, \tag{39e}$$

$$\frac{\alpha^2}{1-\alpha} = 2\frac{s_1}{s_0}\frac{1}{n_{Cs}\rho}\Big(\frac{2\pi m_e kT}{h^2}\Big)^{3/2} e^{-I_1/kT}, \tag{39f}$$

$$n_e = \alpha n_{Cs}, \tag{39g}$$

$$n_k = \rho\frac{m_k}{m_{tot}}\frac{1}{m_k^a}, \tag{39h}$$

$$c_e = \sqrt{\frac{8kT}{\pi m_e}}, \tag{39i}$$

$$q_w = -h(T_s - T_w), \tag{39j}$$

$$T_s = T + \frac{u^2}{2C_{Ar}}, \tag{39k}$$

$$E_y = uB_z(1-K). \tag{39l}$$

5 Numerical Methods

An analytical solution to these equations are difficult to be solved since we cannot decouple the system. Thus to solve this system, a finite difference method over x is

applied down the channel. We use backward difference since this method is known to have absolute stability. Let the spacing over x be defined by x_j, with $i = 0, 1, 2, \cdots, N$ with x_0 being defined as the initial point of the MHD channel, and x_N as the end of the channel. Noting that our 5 variables A, H, T, p, and u are all a function of x we then can discretize our system of equations, defined in equation (37), by the following:

$$\rho_i u_i \frac{u_i - u_{i-1}}{\Delta x} = -\frac{p_i - p_{i-1}}{\Delta x} + j_{y,i} B_z + \mu_i, \tag{40a}$$

$$\rho_i u_i \frac{H_i - H_{i-1}}{\Delta x} = E_{y,i} j_{y,i} - \frac{q_{w,i} C_i}{A_i}, \tag{40b}$$

$$p_i = \rho_i R T_i, \tag{40c}$$

$$T_i = \frac{H_i - \frac{1}{2} u_i^2}{C_{Ar}}, \tag{40d}$$

$$M = u_i / c_{ei}. \tag{40e}$$

Note that any parameter or variable with a subscript i is shorthand for the parameter or variable being evaluated at x_i, that $\Delta x = x_i - x_{i-1}$, and any constants do not have a subscript on them. Also note that all parameters defined in equation (39) are evaluated at x_i.

Before solving the system of equations, there are a few assumptions that will be applied to our system. First we will assume the shape of the channel is square, which implies that $C/A = 4/\sqrt{A}$. We will also always let the magnetic field be 6 Tesla in our simulation [7]. This implies that any time there is seed, or Cesium ion, power

will be extracted. When power is extracted, some sort of energy must be transfered from its current state to electrical energy. We see this energy drop off from thermal and kinetic energy, but when the Mach number is held constant, we see the loss of kinetic energy from a negative pressure gradient down the channel. This is due to the ideal gas law, where pressure is inversely proportional to volume, which is in turn is an increasing function down the channel. Since in application the desire is to let the plasma exhaust travel out into atmospheric conditions, or into a mixing container that will have pressure conditions equal to 1 atmosphere, we will also end our simulated channel wherever 1 atmospheric pressure is achieved. This is to avoid vacuum conditions inside our channel, which would create issues. This implies x_N is never fixed and changes for every case of initial conditions defined in equation (38). Because of this, we have made our step size to be linear and set to $\Delta x = 5 \times 10^{-4}$ m, and can be refined further to achieve sufficient precision.

To solve our system of equations numerically, we use a trust-region-dogleg iterative method, which is the default iterative method in the MATLAB function `fsolve` [2]. This method solves the system of equations by minimizing the sum of the squares using a Gauss-Newton method [2] of $y(z)$, where we define our residuals $y(z)$ to be our system of discretized equations in (40) subtracted all to one side,

$$
\begin{aligned}
y_1(z_i) &= -\rho_i u_i \frac{(u_i - u_{i-1})}{\Delta x} - \frac{p_i - p_{i-1}}{\Delta x} + j_{y,i} B_z + \mu_i, \\
y_2(z_i) &= -\rho_i u_i \frac{(H_i - H_{i-1})}{\Delta x} + E_{y,i} j_{y,i} - \frac{q_{w,i} C_i}{A_i}, \\
y_3(z_i) &= p_i - \rho_i R T_i, \\
y_4(z_i) &= -T_i + \frac{H_i - \frac{1}{2} u_i^2}{C_{Ar}}, \\
y_5(z_i) &= M - u_i / c_{ei},
\end{aligned}
$$

with z being the variables vectorized:

$$
z_i = \begin{bmatrix} u_i \\ H_i \\ p_i \\ T_i \\ A_i \end{bmatrix}. \tag{42}
$$

Note that $y(z)$ is solved to be equal to 0 in the iterative method of `fsolve`. Due to scaling issues of y_2 and y_4, and nonlinearity issues in y_3, adjustments had to be implemented. Note that since these are going to be set to zero through iteration, any variables, parameters, or constants multiplied to $y(z)$ can be disregarded. To scale y_2 and y_4, we multiply through by constants Δx and C_{Ar}, respectively. Note that $y_5(z_i)$ is nonlinear, but since T_i is on the magnitude of $1,000$, there are no issues, and we

cannot remove the nonlinearity due to the square root function. In addition, although equation y_3 appears linear, it is nonlinear due to the conservation of mass equation (22) that holds ρ to be inversely proportional to both u and A, and more importantly, the area of the channel can be very close to 0. Also note this is not an issue in y_2 due to the magnitude of H_i. To resolve this, we plug in ρ from the conservation of mass equation and multiply through by its denominator, thus making the residuals to be:

$$y_1(z_i) = -\rho_i u_i \frac{(u_i - u_{i-1})}{\Delta x} - \frac{p_i - p_{i-1}}{\Delta x} + j_{y,i} B_z + \mu_i, \tag{43a}$$

$$y_2(z_i) = -\rho_i u_i (H_i - H_{i-1}) + E_{y,i} j_{y,i} \Delta x - \frac{q_{w,i} C_i}{A_i} \Delta x, \tag{43b}$$

$$y_3(z_i) = A_i u_i p_i - \dot{m} R T_i, \tag{43c}$$

$$y_4(z_i) = -C_{Ar} T_i + H_i - \frac{1}{2} u_i^2, \tag{43d}$$

$$y_5(z_i) = M - u_i / c_{ei}. \tag{43e}$$

This set of equations is solved sequentially at x_i for every $i = 1, 2, ..., N$ with the initial conditions at x_0 given in (38), with $x_N = \{x_i \mid p_i \leq 1 \text{ atm}\}$.

One last thing to note is that typically, one can implement the Jacobian to speed up the solver because it is solved numerically in each step, but this is difficult to implement in our numerical solver. This is due to the severe nonlinearity with temperature, which can be seen in the conduction current term j. In j, the nonlinearity of temperature is a seen due to the dependence of conductivity and Saha equation. This would

make any finite difference gradients required to set the Jacobian very computationally expensive and error prone, thus they will be solved by iterative methods.

6 Numerical Solution

The numerical solution depicted in Figure 1 of this system of equations follows that of what is expected. The pressure decreasing over time, along with the temperature, implies that the velocity should drop as well to keep the Mach number constant from $y_5(z)$. Note that it makes sense that the amount of energy is decreasing over time, as seen in the enthalpy. Also see that conductivity is related to the growth of electron mobility μ_e and the decay in the number of electrons n_e, and since the conductivity is increasing, it shows that the electron mobility is more dominant. There two possible outcomes expected when extracting power – either the pressure decays to 1 atm due to extraction of kinetic energy, or the conductivity decreases to 0 due to the decrease in the number of free electrons. In Figure 1, the conductivity is still increasing, so there implies a need for an optimization problem of efficiency under constraints, where

$$\text{Eff} = \frac{P_{out}}{P_{in}} = \frac{-1}{\dot{m}\big(H_0 + 1/2\ u_0^2\big)} \int_{x_0}^{x_N} E_y\ j_y A\ dx. \tag{44}$$

The optimization method will be further defined in the optimization section, but the efficiency is noted here to show the significance. For example, the particular channel in Figure 1 with initial conditions $M = 2.5$, $T_0 = 2500$ K, $p_0 = 2.5 \times 10^6$ atm, $\dot{m} = .1$ kg/s/m^3, and $n_{Cs} = .02\ n_{tot}$ has an efficiency of 3%, which is very small.

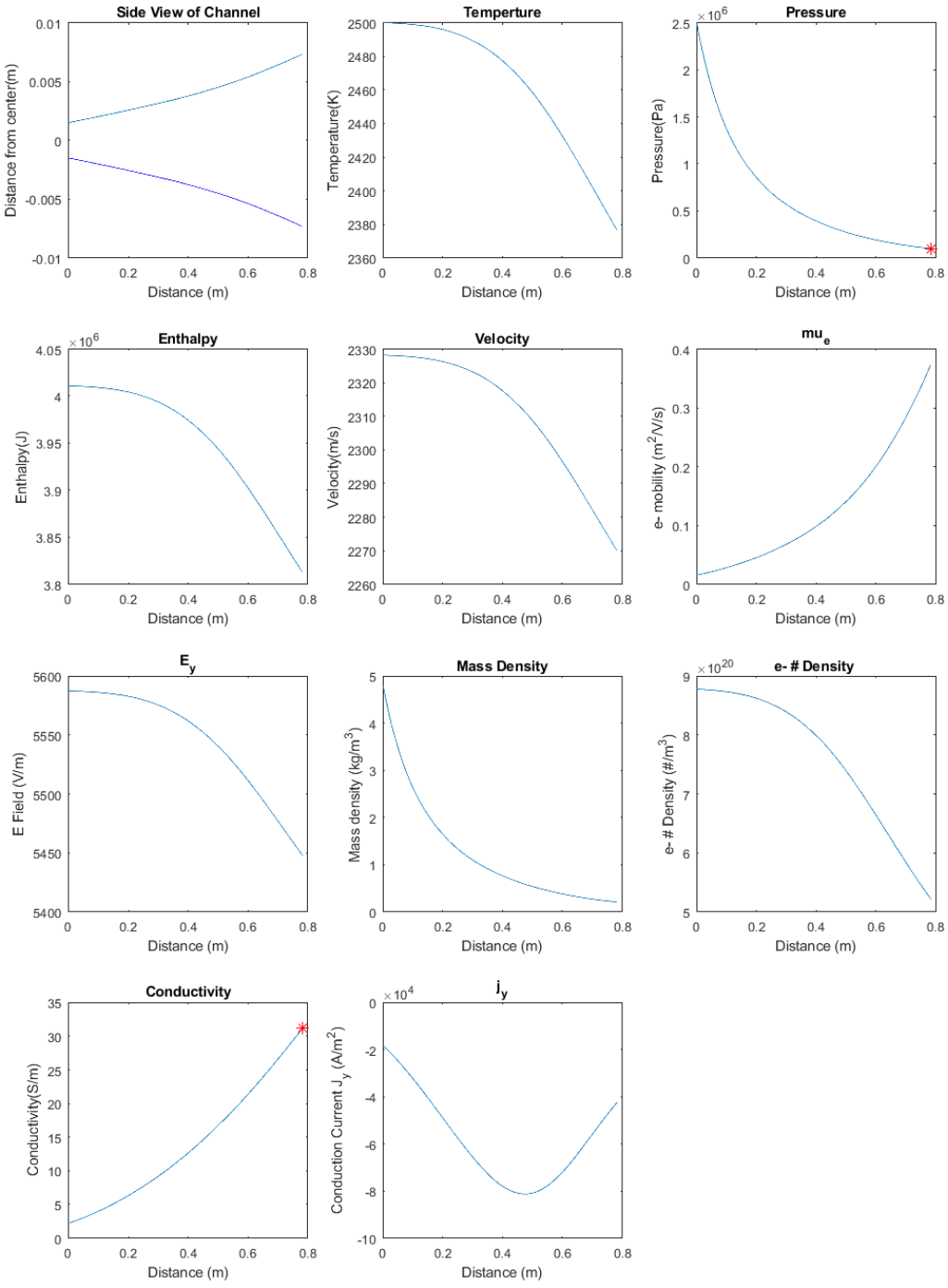

Figure 1: Shows the properties down the distance of the channel of an 1D steady state MHD generator with initial conditions $M = 2.5$, $T_0 = 2500$ K, $p_0 = 2.5 \times 10^6$ atm, $\dot{m} = .1$ kg/s/m^3, and $n_{Cs} = .02\ n_{tot}$. Note that the red star on the pressure and conductivity plots are where pressure is less than 1 atm as a check to ensure it occurs at the end of the channel. This specific channel has an efficiency of about 3%.

Since the iteration method is only an approximation to the true solution, error analysis was conducted on our 5 variables in our vector z for validation in our numerical solution. MATLAB results show us that our $y(z)$ does in fact converge to zero, with $||y_i(z)||_2 \leq 10^{-3} = \tilde{y}_{tol}$. The issue is that we want to find the error of z without knowing the true solution z^*. To conduct this analysis, we had the system of equations $y_i(\tilde{z})$ solved for each spatial step. We then set a lower tolerance on $y_i(z)$ denoted as y_{tol} with solution z and have the simulation take a maximum (set arbitrarily) of 3 more iterative steps to represent a more true solution to the system of equations. Then we calculated the difference between these 2 terms and called it an estimate of our error for each spatial step [1, p. 69],

$$\delta z_i = ||z_i - \tilde{z}_i||_2 \approx ||z_i^* - z_i||_2. \tag{45}$$

From this, we created confidence regions defined as:

$$\text{conf}(x_i) = z(x_i) \pm \sum_i \delta z(x_i), \tag{46}$$

to visually represent the accumulation of numerical error on each spatial step, seen in Figure 2. As seen in the figure, the confidence regions completely hide the solution z , showing that the accumulation error is nearly nonexistent. When calculating the relative error at x_N since this is the spatial step where the most error has accumulated,

or

$$\frac{||\text{conf}(x_N) - z(x_N)||_2}{||z(x_N)||_2},$$

this is on the order of magnitude of 10^{-10}, showing the precision of the solution.

To compare the precision of our result to something else, we made a numerical model that allowed the Mach number to vary down the channel with a set fixed geometry, and found the confidence regions of this simulation, shown in Figure 3. When doing this, we found a much larger confidence region, with the maximum relative error being about 16% at the end of the channel, denoted by a green star. This comparison shows that for the sole purpose of precision, the fixed Mach number simulation is much better than the fixed geometry or area simulation.

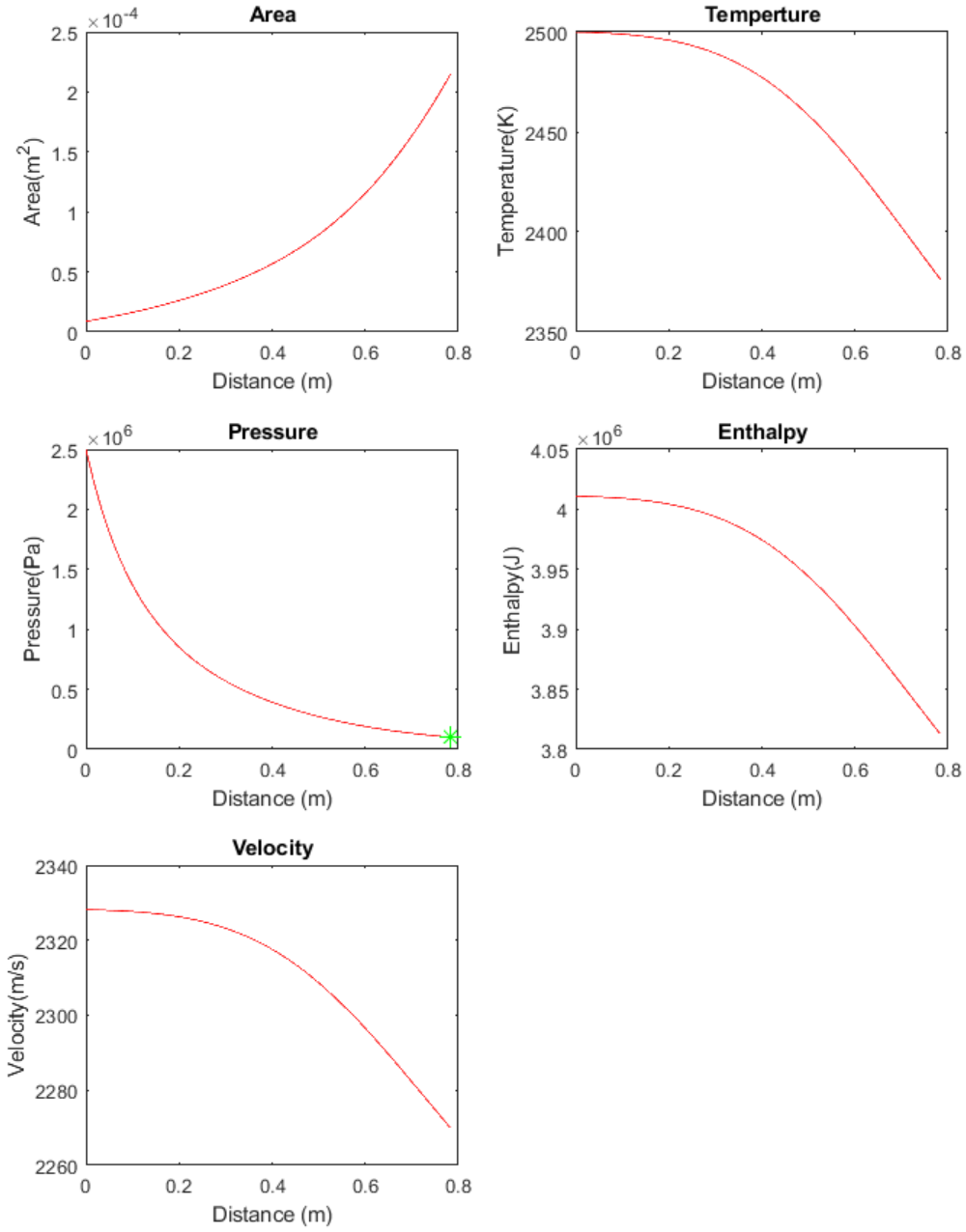

Figure 2: Shows the confidence region down the distance of the channel of an 1D steady state MHD generator with initial conditions $M = 2.5$, $T_0 = 2500$ K, $p_0 = 2.5 \times 10^6$ Pa, $\dot{m} = .1$, and $n_{Cs} = .02\ n_{tot}$. Note that the green star on the pressure and plot is where pressure is less than 1 atm as a check to ensure it occurs at the end of the channel. The confidence bands shown in red, are so close to the solution that they cannot be distinguished from each other, implying our solution is precise. The relative error at x_N is 2.25×10^{-10}.

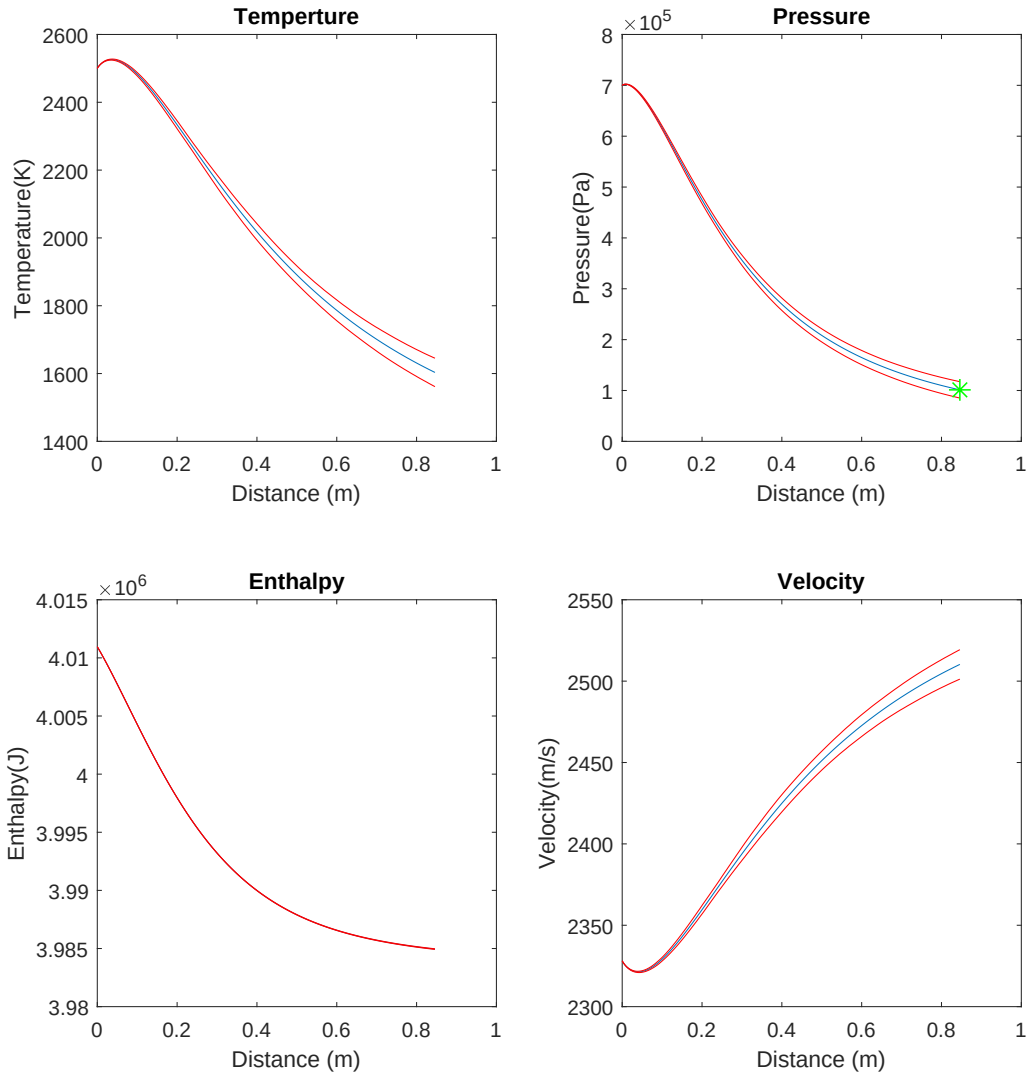

Figure 3: Shows the confidence region down the distance of the channel of an 1D steady state MHD generator with the a fixed channel geometry (Mach number and mass flow rate allow to vary) with initial conditions $M = 2.5$, $T_0 = 2500$ K, $p_0 = 7 \times 10^5$ Pa, $A_0 = .0005$, and $n_{Cs} = .02\ n_{tot}$. Note that the green star on the pressure and plot is where pressure is less than 1 atm. The confidence bands shown in red, are close to the simulated best result, but are distinguishable. At $x_N = \{x_i |\ p = 1 \text{ atm}\}$, the maximum relative error on the 4 variables is 16%.

7 Optimization of Efficiency

As previously noted in the simplified MHD equation section and the numerical solution section, initial conditions for the system need to be determined optimally. In applications of an MHD generator such as implementation into a coal or natural gas power plant system, efficiency of the generator is the desired parameter to optimize, with benefits of either increasing profit or reduce carbon emissions for power companies. Let power efficiency be defined again by equation (44),

$$\text{Eff} = \frac{P_{out}}{P_{in}} = \frac{-1}{\dot{m}\big(H_0 + 1/2\ u_0^2\big)} \int_{x_0}^{x_N} E_y\ j_y A\ dx,$$

where the initial power is defined as $\dot{m}\big(H_0 + 1/2\ u_0^2\big)$, or the sum of thermal and kinetic energy at the initial condition or the start of the magnetic field, and the power out is described as the the negative integral over volume of power going out of the system.

The optimization problem will be defined by some parameters that can be controlled through manipulation of geometry of the channel. In our numerical solution, the geometry of the channel is calculated according to the area's spatial dependence of the Mach number, along with dependence on the initial conditions. This implies that the optimization of efficiency should be dependent on the initial conditions of the simulated MHD channel. Let us define the efficiency optimization problem to be

$$\text{Eff}_{max} = \max_{M,\ p_0,\ T_0,\ \dot{m},\ \frac{m_{Cs}}{m_t ot}} \left(\frac{-1}{\dot{m}\big(H_0 + 1/2\ u_0^2\big)} \int_{x_0}^{x_N} E_y\ j_y A\ dx \right). \tag{47}$$

We must also take into account for the physical constraints on the conditions we are optimizing over. As discussed before, we want to follow the approach where the speed in the channel is greater than the speed of sound in the channel, or $M \geq 1$. Due to engineering constraints, we also want an upper bound of $M \leq 5$. Pressure would be bounded below by 1 atm (or 101,325 Pa) since pressure decreases as power is extracted and our channel is set to end wherever 1 atm is achieved. The upper bound on pressure will be arbitrarily set to be 10^7 Pa (about 100 atm) due to stress on the channel - which would need to be adjusted according to a number of factors, such as material and thickness of the material, to ensure safety. We will let the temperature be bounded above arbitrarily by 5000 K, which would need to be adjusted according to fuel being burned, or bounded by 8000 K due to issues that could arise in the Saha equation (33). We will also arbitrarily set the bounds of the mass flow rate with $.01 \leq \dot{m} \leq 1000$, which may be adjusted according to stress implemented on channel and a number of other factors. Lastly, we will bound the percentage of seed in the system below by 0, and bound it arbitrarily above by .1 to ensure the approximation of removing the electron ion collision term is held, which has been removed solely for the purpose of the optimization due to issues with the efficiency when included. To conclude, the constraints they are provided below:

$$1 \leq M \leq 5,$$

$$101325 < p_0 \leq 10^7,$$

$$1000 \leq T_0 \leq 5000,$$

$$.01 \leq \dot{m} \leq 1000,$$

$$0 \leq \frac{m_{Cs}}{m_tot} \leq .05.$$

To understand a rough approximation of the location of the optimal conditions, and a rough estimation of which constraints are active or inactive, 2D surfaces and 1D plots have been generated with other optimization parameters fixed. Note that the figures are not a perfect representation of which constraints are active since there is interdependence of the 5 variables (for example, Mach number is dependent on temperature). These figures are shown in Figure 4.

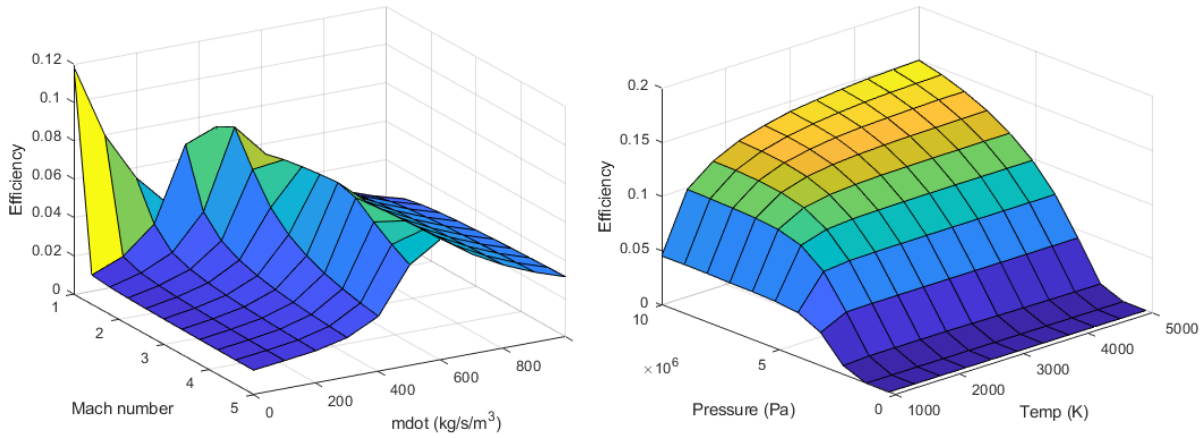

(a) (b)

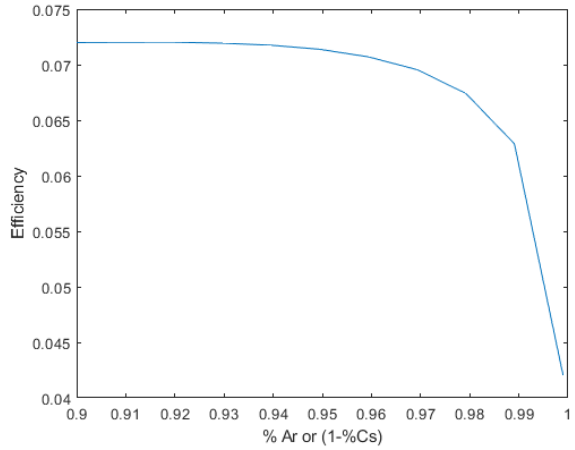

(c)

Figure 4: (a) Shows the efficiency as a function of Mach number and mass flow rate while temperature, pressure, and seed percentage are fixed. (b) Shows the efficiency as a function of initial pressure and temperature with a fixed Mach number, mass flow rate, and seed percentage. (c) Shows the efficiency as a function of 1 minus the seed input percentage.

Results in these show that the upper constraints on pressure and temperature from figure 4b are expected to be active, and the upper constraints on seed, Mach number, and mass flow rate, along with the lower constraints on pressure and temperature, are inactive. We see that there seems to be a possible sensitive peak around low Mach number and low mass flow rate from Figure 4a, and another peak around $M \approx 2$ and $\dot{\mathbf{m}} \approx 500$, implying that the location of the initial guess may be a factor in the numerical constrained optimization. Lastly, we see in Figure 4c that the effect of seed percentage seems as if there is little to no effect on the optimization for percentages between 5-10%. It would be ideal to use less seed since it makes the negation of the electron ion collision term more exact, and to decrease cost of seed in application, so we will adjust the upper bound on the seed to be about 5% .

The constrained numerical optimization was completed on MATLAB using the function `fmincon`, which is a nonlinear minimization solver that allows for constraints. Note that we adjusted the problem to minimize for the negative efficiency, or equivalently, to find the maximum. The results to the optimization are held below:

Table 1: Shows the optimal parameters and initial conditions that give the maximum efficiency with drag loss effects.

Optimal values					
M^{opt} [1]	p_0^{opt} [Pa]	T_0^{opt} [K]	$\dot{\mathbf{m}}^{opt}$ [kg/s/m^3]	%Cs^{opt} [1]	Eff$_{max}$ [1]
1.5936	10^7	5000	400	5%	26.18%

For the most part, these results seem to closely follow that expected by analyzing the constraints in Figure 4. To understand the impact this could make – assuming

the chemical species were combustion products (which they are not in our case), and assuming the implementation into a 40% efficient power plant, this would increase its efficiency to about 56%, which would have a huge effect on the both the amount of carbon emitted and the energy production the plant would have.

8 Conclusion

The generalized MHD model was simplified to receive a steady-state 1-dimensional MHD problem with a chemical composition of Argon and Cesium. This model was then numerically set up and solved with the Mach number held constant, and optimized to find the best initial conditions under constraints that would maximize the efficiency of an MHD generator with the given chemical composition to about 26%. While the Argon-Cesium composition is not comparable to that of combustion system, one would only need to (1) adjust the conductivity for the whole system of chemical species that occur in the intermediate steps of combustion, (2) adjust the Saha equation to a system since there is a possibility of multiple ions such as OH^- and H^+, and (3) re-optimize with properly adjusted constraints.

Further analysis could also be done on this research by adjusting the Saha equation and optimizing with temperature above the 8,000 K bound set in our problem. One could also optimize profit for power companies, which would include price for both seed and the superconducting magnet needed. The system could be adjusted to allow for motion in a radial direction from the center of the channel, which would change the

system into a steady-state, 2-D stationary problem. Additionally, one could remove the assumptions and simplifications on the drag and heat transfer to understand their true effect, or remove the assumption supplied by Rosa et al. and to optimize the efficiency as a function of the geometry of the channel.

Acknowledgements

This research was supported in part by an appointment to the U.S. Department of Energy (DOE) Professional Internship Program at the National Energy Technology Laboratory administered by the Oak Ridge Institution for Science and Education. I also want to note the mentorship of Professor Nathan Gibson, along with the help of Dr. Rigel Woodside, Hyoungkeun Kim, and David Huckaby throughout this project.

References

[1] C. T. Kelley. *Iterative Methods for Linear and Nonlinear Equations*. Society for Industrial and Applied Mathematics, Philidelphia, PA, 1995.

[2] MATLAB. *Equation Solving Algorithms*. The MathWorks Inc., Natick, Massachusetts, 9.3.0.713579 (r2017b) edition, 2006.

[3] P. M. Morse and H. Feshbach. *Methods of Theoretical Physics*, volume 22. AAPT, 1953.

[4] R. J. Rosa. *Magnetohydrodynamic Energy Conversion*. Hemisphere Publishing, New York, NY, 1987.

[5] E. J. Sheppard. *Ionization Nonequilibrium and Ignition in Plasma Accelerators*. PhD thesis, Massachusetts Institute of Technology, 1994.

[6] G. W. Sutton and A. Sherman. *Engineering Magnetohydrodynamics*. Courier Dover Publications, 2006.

[7] C. Woodside. Retrospective and prospective aspects of mhd power generation. Presentation at NETL/DOE MHD Workshop, Arlington, VA, 2014.